Bandwidth Optimization by Dielectric Loading

SHALOM HALEVY, SHALOM RAZ, AND HAIM CORY

Abstract—**The known theory of dielectrically loaded rectangular waveguides is combined with appropriate optimization procedures to yield optimal bandwidth design. The minimal acceptable power handling capacity and/or the maximal allowed losses are used as constraints. Alternatively, power handling capacity or losses may be considered as the desired optimization targets. The numerical determination of the relevant cutoff frequencies is carried out by the efficient mode-matching technique as well as the more generally applicable moment solution. Alternative search algorithms are used and compared. Results of the optimization process are given a simple physical interpretation.**

I. Introduction

THE DIELECTRIC loaded waveguide has long been recognized as an attractive propagation medium, possessing desirable features such as substantially increased bandwidth and power handling capacity. The associated propagation features, particularly for stratified loading, have been thoroughly investigated and are well known [1]–[4].

A primary objective of this paper is to combine the known theory of stratified loaded guides and the associated numerical capability with appropriate optimization schemes. We present a procedure yielding optimal bandwidth design with minimal power handling capacity and/or maximal allowed losses as constraints. Alternatively, power handling capacity or losses may be selected as the desired optimization targets with, for example, the bandwidth as a constraint.

The useful frequency band is, in principle, given by $\omega_d < \omega < \omega_{sd}$, where ω_d and ω_{sd} denote the cutoff frequencies of the first (dominant) mode (LSE_{01} in the configuration of Fig. 1), and the second (subdominant) mode (LSE_{02}, LSE_{11}, or LSM_{11} depending upon the waveguide and loading parameters in the configuration of Fig. 1 [3]).

The numerical determination of the relevant cutoff frequencies and field distribution is carried out by both the classical and efficient (whenever applicable) mode-matching technique [2] and by the more general moment method [5]. The optimization sequence was carried out by two alternative search algorithms suggested by [6] and [7], of which the first has consistently been found to be more efficient.

The bandwidth extension mechanisms are discussed from the point of view of perturbation theory in Section II. Perturbation arguments help clarify some of the basic trends, e.g., the fact that maximal influence on the cutoff frequencies is obtained by dielectric loading of regions of maximal (modal) electric fields while modes characterized by vanishing electric fields in the loaded region remain essentially unaffected.

Manuscript received September 12, 1977; revised January 20, 1978.

The authors are with the Department of Electrical Engineering, Technion—Israel Institute of Technology, Haifa, Israel.

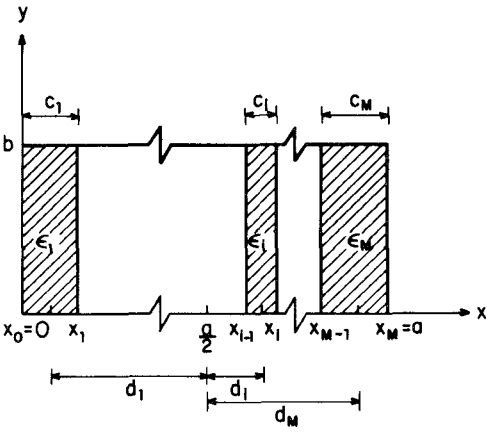

Fig. 1. Rectangular waveguide loaded with M dielectric slabs.

The analytical and numerical aspects are described in Section III. No difficulties are encountered in the application of the mode-matching technique. A convergence difficulty arose in applying the moment solution to LSM modes. This difficulty, traceable to the appearance of discontinuities in the modal fields, was resolved by an appropriate choice of hybrid basis.

The specific configuration of a single centrally situated slab and its unconstraint optimization is discussed in Section IV-A. In Section IV-B, the authors also address the asymmetrical and multi-slab configurations (Fig. 1) from the viewpoint of the role that the added parameters (degrees of freedom) can play in the optimization process. Section IV-C deals with the problem and conclusions of constraint optimization. For reasons exhibited in Section IV-B, only the symmetric single-slab configuration is discussed in this context.

II. Theoretical Considerations

Let us consider an infinitely long dielectrically loaded rectangular waveguide having perfectly conducting walls. It is assumed that the guide's width a in the x direction, is larger than or equal to its height b in the y direction. It is further assumed that the relative permittivity ϵ is x dependent only, and that the relative permeability $\mu = 1$. The electromagnetic (EM) fields propagating in this guide could be classified into LSE modes ($E_x = 0$) and LSM modes ($H_x = 0$), which constitute a complete set.

0018-9480/78/0600-0406$00.75

A. The LSE and LSM Modes

The electric and magnetic fields of the ith LSE mode are derivable from a Hertz magnetic vector potential given by [2], [8]

$$\Pi_{hi} = \bar{a}_x \phi_{hi}(x) \cos \frac{m\pi y}{b} \exp(-j\beta_i z), \qquad m = 0, 1, 2, \cdots. \tag{1}$$

$\phi_{hi}(x)$ satisfies the following differential equation:

$$-\frac{d^2\phi_{hi}(x)}{dx^2} + \left\{\left(\frac{m\pi}{b}\right)^2 + \beta_i^2\right\}\phi_{hi}(x) = \epsilon(x) k_0^2 \phi_{hi}(x) \tag{2}$$

and boundary conditions

$$\phi_{hi}(0) = \phi_{hi}(a) = 0. \tag{3}$$

Similar considerations apply for the LSM modes [2], [8].

B. Mode Classification and Bandwidth Definition

There is a double infinity of solutions for each mode type, to be denoted as LSE_{mn} and LSM_{mn}. The index m refers to the y dependence of the potential, while the index n is related to the x domain eigenfunction having the eigenvalue $\omega_{c,n}$: $(\omega_{c,n} \geqslant \omega_{c,n-1})$. These eigenvalues, i.e., the cutoff frequencies, are found by setting $\beta = 0$ in the differential equations of the modes, and solving the resulting equations by the numerical methods described in the next paragraph. LSE_{01} will retain its dominant mode role throughout. From the properties of the Sturm–Liouville operator [9], it appears that the eigenvalues of the $LSE_{mn}(LSM_{mn})$ modes are lower than the eigenvalues of the $LSE_{m'n'}(LSM_{m'n'})$ modes, if $m = m'$ and $n < n'$, or if $n = n'$ and $m < m'$, or if $m < m'$ and $n < n'$. Therefore, the modes "competing" for second place are LSE_{02}, LSE_{11}, and LSM_{11}, and only these modes need to be considered in the bandwidth optimization problem. The second-place mode will be referred to as the "subdominant mode."

We shall define the cutoff frequency ratio (CFR) as follows:

$$\mathrm{CFR} = \omega_c / \omega_d \tag{4}$$

where ω_d is the cutoff frequency of the dominant (LSE_{01}) mode, while ω_c is the cutoff frequency of any other mode. The CFR of the subdominant mode will be termed bandwidth (BW).

$$\mathrm{BW} = \frac{\omega_{sd}}{\omega_d}. \tag{5}$$

Alternative bandwidth definitions are possible, but the above definition is the simplest and most usual one. It is noted that for a waveguide completely filled with a homogeneous dielectric, the subdominant mode is the $LSE_{02}(TE_{20})$ in the range $0 < b/a \leqslant 1/2$, with $\mathrm{BW} = 2$, while in the range $1/2 \leqslant b/a \leqslant 1$, the subdominant mode is the $LSM_{11}(TE_{01})$ with $\mathrm{BW} \leqslant 2$.

C. Bandwidth Improvement and the Perturbation Method

The tendencies of bandwidth improvement can be studied by performing a small perturbation in the fully loaded guide's geometry and/or its loading, and calculating the results bandwidth. In the $0 < b/a \leqslant 1/2$ range, we have either to lower the cutoff frequency of the LSE_{01} mode or to raise the cutoff frequency of the LSE_{02} mode. Clearly, the perturbation method could only hint at the initial bandwidth response to the guide's parameters variation.

Let us consider an infinitely long cylindrical waveguide of cross section S with perfectly conducting walls, completely filled with a dielectric of relative permittivity ϵ and permeability μ, and let $(\bar{E}_0, \bar{H}_0)$ denote the presumedly known fields at cutoff (ω_{c0}).

If we perform a perturbation ΔS in the waveguide's cross section, we shall obtain the following approximate expression for the relative bandwidth [10]:

$$\frac{\omega_c - \omega_{c0}}{\omega_c} \cong \frac{\int_{\Delta S}\int \left(\mu \bar{H}_0 \cdot \bar{H}_0^* - \epsilon \bar{E}_0 \cdot \bar{E}_0^*\right) dS}{\int_S \int \left(\mu \bar{H}_0 \cdot \bar{H}_0^* + \epsilon \bar{E}_0 \cdot \bar{E}_0^*\right) dS} \tag{6}$$

where ω_c is the cutoff frequency in the perturbed configuration. Therefore, an inward perturbation will decrease *or* increase the cutoff frequency if it is made at a location where the electric *or* the magnetic fields, respectively, are highest. An application of this effect for increasing the bandwidth could be found in ridge waveguides.

If the perturbation is performed in the dielectric parameters, the following approximate expression for the relative bandwidth [10] will be obtained:

$$\frac{\omega_c - \omega_{c0}}{\omega_c} \cong -\frac{\int_S \int \left(\Delta\epsilon \bar{E}_0 \cdot \bar{E}_0^* + \Delta\mu \bar{H}_0 \cdot \bar{H}_0^*\right) dS}{\int_S \int \left(\epsilon \bar{E}_0 \cdot \bar{E}_0^* + \mu \bar{H}_0 \cdot \bar{H}_0^*\right) dS} \tag{7}$$

where $\Delta\epsilon$ and $\Delta\mu$ are local changes in the relative permittivity and permeability, respectively. Therefore, an increase in ϵ or μ will decrease the cutoff frequency. An application of this effect for increasing the bandwidth has been proposed in [1] and [3]. Let us consider a centrally loaded waveguide with a thin dielectric slab of width c $(c \ll a)$ and permeability ϵ $(\epsilon \gtrsim 1)$. Since the electric field $\bar{E}_0$ in the central region of the empty guide is maximal for the LSE_{01} (dominant) mode and essentially zero for the LSE_{02} mode, we infer from perturbation theory that the cutoff frequency of the first mode will decrease while that of the second mode will remain essentially unaffected by the proposed perturbation. Vartanian [1] has pointed out several practical reasons for which permittivity changes are preferable to cross-section modifications as long as dielectric losses stay acceptably small. Therefore, this paper deals exclusively with dielectric relative permittivity perturbations $(\epsilon = \epsilon(x))$ for bandwidth (constraint and unconstraint) optimization purposes.

III. Numerical Solution of the Wave Equation at Cutoff and Bandwidth Optimization

Consider a waveguide loaded with M dielectric slabs of width c_i, relative permittivity ϵ_i, and relative permeability unity, as shown in Fig. 1.

In this section, we describe alternative numerical methods used for finding the cutoff frequencies of the above-mentioned configuration: the field-matching method [2] and the moment method [5], [11]. We shall describe afterwards the optimization method used to obtain the optimal bandwidth.

A. The Field-Matching and Moment Methods

In the field-matching method, the cutoff frequencies of the LSE modes are given by the roots of the element $F_{12}(\omega)$ of the following matrix [3]:

$$F=\prod_{i=1}^{M} T_i \tag{8}$$

where

$$T_i=\begin{bmatrix} \cos p_i c_i & (\sin p_i c_i)/p_i \\ -p_i \sin p_i c_i & \cos p_i c_i \end{bmatrix} \tag{9}$$

$$p_i^2=\epsilon_i k_0^2-\left(\frac{m\pi}{b}\right)^2. \tag{10}$$

The cutoff frequencies of the LSM modes could be found in a similar manner [3].

In the moment method (Galerkin choice), the desired cutoff frequencies are given by setting the following determinant to zero:

$$\det\left\{[l_{ij}]-k_0^2[m_{ij}]\right\}=0 \tag{11}$$

where

$$l_{ij}=\int_0^a Lf_i \cdot f_j\,dx \tag{12}$$

$$m_{ij}=\int_0^a Mf_i \cdot f_j\,dx. \tag{13}$$

For the LSE modes

$$L=-\frac{d^2}{dx^2}+\left(\frac{m\pi}{b}\right)^2 \tag{14}$$

$$M=\epsilon(x) \tag{15}$$

and $f_i(x)$ are prescribed basis functions satisfying, separately, the required boundary conditions.

The cutoff frequencies of the LSM modes could be found in a similar manner.

B. Convergence of the Moment Method

The degree of accuracy of the moment method is difficult to ascertain. In order to determine its convergence properties, we have compared it with the field-matching method (henceforth the "exact solution") which, whenever applicable, may yield solutions to any desired accuracy.

The convergence properties of the moment solution were tested for a single centered slab configuration. Appropriate basis functions were chosen for each mode, taking advantage of the relevant symmetry properties. We have considered *harmonic* basis functions, which coincide with the eigenfunctions of the modes propagating in the empty waveguide as well as the *polynomial* basis functions shown in Table I.

TABLE I
HARMONIC AND POLYNOMIAL BASIS FUNCTIONS

Mode	Harmonic Set	Polynomial Set
LSE_{01}, LSE_{11}	$\sin i\pi x$ $(i = 1,3,5,\ldots)$	$(2x-1)^{2i}-1$, $(i = 1,2,3,\ldots)$
LSE_{02}	$\sin i\pi x$ $(i = 2,4,6,\ldots)$	$(2x-1)((2x-1)^{2i}-1)$, $(i = 1,2,3,\ldots)$
LSM_{11}	$\cos i\pi x$ $(i = 0,2,4,\ldots)$	1 $(i = 1)$ $(2x-1)^{2i}-i(2x-1)^2$, $(i = 2,3,4,\ldots)$

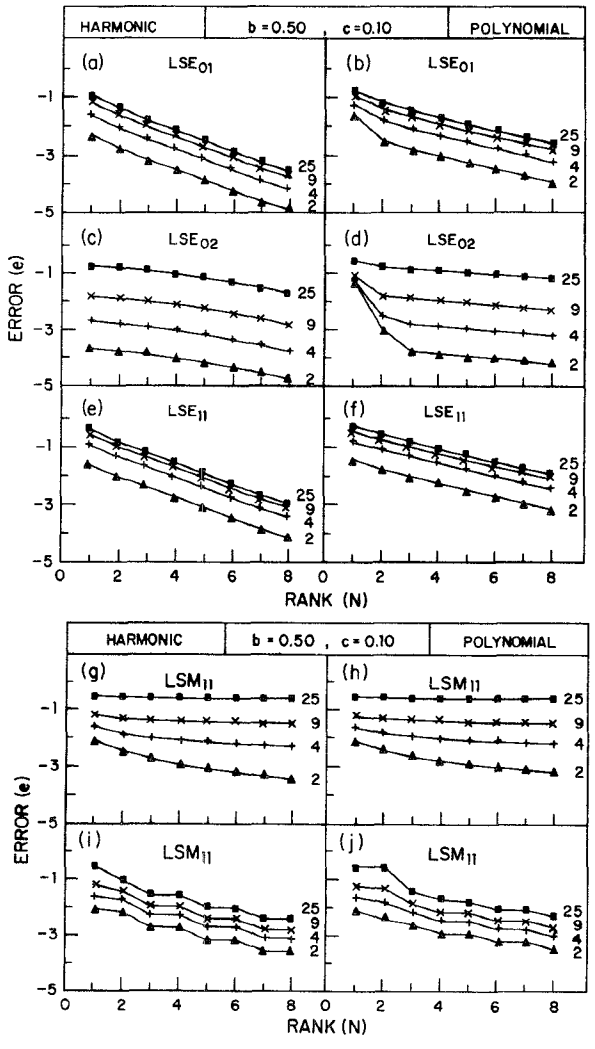

Fig. 2. Convergence error for harmonic and polynomial sets versus rank.

Let us denote the "exact" eigenvalue by ω_c, the moment solution of rank N by $\omega_{c,N}$, and the error measure by

$$e\equiv\log_{10}\frac{\omega_{c,N}-\omega_c}{\omega_c}. \tag{16}$$

The Galerkin choice guarantees convergence from above ($\omega_{c,N}>\omega_c$) for symmetric, positive definite operators [12]. The convergence error for harmonic and polynomial sets of functions is described for the four modes of interest in Figs. 2(a)–(h) as a function of the rank N for $b=0.50$, $c=0.10$, and with the slab's relative permittivity (ϵ) as

parameter. Convergence errors have also been calculated for other parametric values, leading to similar conclusions.

For the LSM_{11} mode, especially at higher values of ϵ, the moment solution has exhibited poor convergence properties, even with $N=50$ for the harmonic set. The poor convergence of the procedure for LSM modes has been traced back to the discontinuous nature of $d\phi_{ei}/dx$ at the slab's boundaries where $\phi_{ei}(x)$ represents the x dependence of the appropriate electric vector potential. The continuous basis could not describe accurately the discontinuous region. This difficulty was overcome by adding another set of functions which facilitated an efficient and simple description of the discontinuity.

Define two sets of *harmonic* basis functions as follows ($a=1$):

$$e_i(x)=\cos i\pi x, \qquad x_0\leqslant x\leqslant x_3, \quad i=0,2,4,\cdots \tag{17}$$

$$h_i(x)=\begin{cases}\sin i\pi((x-x_1)/(x_2-x_1)), & x_1\leqslant x\leqslant x_2\\ & i=1,3,5,\cdots\\ 0, & x_0\leqslant x\leqslant x_1,\ x_2\leqslant x\leqslant x_3\\ & i=1,3,5,\cdots.\end{cases} \tag{18}$$

The basis functions $e_i(x)$ are, as before, the eigenfunctions of the LSM mode in the empty waveguide, and the basis functions $h_i(x)$ are the eigenfunctions of the LSE mode in a waveguide stretching from x_1 to x_2 (Fig. 1). The derivatives of $h_i(x)$ and $\phi_e(x)$ have discontinuities at the same points. It may be anticipated that the following hybrid basis would improve the convergence substantially:

$$f_1=e_0, f_2=h_1, f_3=e_2, f_4=h_3,\cdots. \tag{19}$$

A similar double set of *polynomial* basis functions has also been considered ($a=1$):

$$e_i(x)=\begin{cases}1, & i=1\\ \xi^{2i}-i\xi^2, & i=2,3,4,\cdots\end{cases} \tag{20}$$

$$h_i(x)=\begin{cases}0, & x_0\leqslant x\leqslant x_1,\ x_2\leqslant x\leqslant x_3, \quad i=1,2,3,\cdots\\ \xi^{2i}-1, & x_1\leqslant x\leqslant x_2, \quad i=1,2,3,\cdots\end{cases} \tag{21}$$

where

$$\xi\equiv\frac{2x}{x_1+x_2}-1$$

and

$$\xi\equiv\frac{\xi}{x_2-x_1}$$

and the hybrid basis

$$f_1=e_1, f_2=e_2, f_3=h_1, f_4=e_3, f_5=h_2, f_6=e_4,\cdots \tag{22}$$

has been tested. The convergence error for the new harmonic and polynomial sets is given in Figs. 2(i) and (j) as a function of the rank with $b=0.50$, $c=0.10$, and ϵ as parameter.

The following conclusions can be drawn from the convergence analysis.

1) The polynomial set is found to be generally inferior to the harmonic basis in accuracy, rate of convergence, simplicity, and efficiency of the computation.

2) For given c and N, the error increases as ϵ and/or $(m\pi/b)^2+\beta^2$ increase, for all modes.

3) A considerable improvement of the convergence rate for LSM modes is achieved, especially for higher ϵ, via the use of a hybrid basis possessing appropriate derivative discontinuities.

C. The Optimization Method

The bandwidth function $BW(b,\epsilon(x))$ is calculated numerically. If the (constraint or unconstraint) extremum of this function is to be found, an optimization scheme is preferred which does not require the numerical computation of the derivative. The Powell [6] the Nelder–Mead [7] algorithms were used and found quite satisfactory. The former has generally exhibited better convergence properties. In either case, we have obtained faster convergence by optimizing BW^2 rather than BW.

IV. Discussion and Interpretation of the Results

A. Single Dielectric Slab

According to perturbation theory (Section II), insertion of a dielectric slab in a rectangular waveguide may improve its bandwidth. In this section, the influence of the guide's geometry and dielectric slab loading on the cutoff frequency ratios of the relevant modes and consequently on the bandwidth is investigated. Optimal bandwidth solutions are found for the centrally loaded single-slab configuration. For convenience, and without loss of generality, $a=1$. All computations in this chapter were carried out via both mode-matching and moment techniques.

Graphs of the ratio of the cutoff frequency of a centrally loaded guide to that of an empty one (ω_c/ω_e) are given in Figs. 3(a)–(d) for LSE_{01}, LSE_{02}, LSE_{11}, and LSM_{11} modes as a function of the slab's width c with the relative permittivity ϵ as parameter, and guide heights b of 0.50 and 0.40. As can be anticipated, the cutoff frequencies of the LSE_{01} and LSE_{02} modes for the loaded and empty waveguides do not depend on b, while those of the LSE_{11} and LSM_{11} do.

It can be seen from the graphs that, for given ϵ and c, the influence of the slab's presence is felt, in decreasing order of importance, by the modes LSE_{11}, LSE_{01}, LSM_{11}, and LSE_{02}. The cutoff frequencies of all the modes decrease for increasing ϵ and c and increase for increasing b.

Graphs of the cutoff frequency ratios (ω_c/ω_d) dependence on c are given in Figs. 4(a)–(c) for LSE_{02}, LSE_{11}, and LSM_{11} modes.

The following conclusions can be drawn. For all three modes, CFR increases and approaches an asymptotic value, for given c and b, as ϵ increases. The slab's width c corresponding to an extremum in bandwidth decreases, for a given b, as ϵ increases. For given ϵ and b, CFR possesses a maximum for LSE_{02} and LSM_{11} modes and a

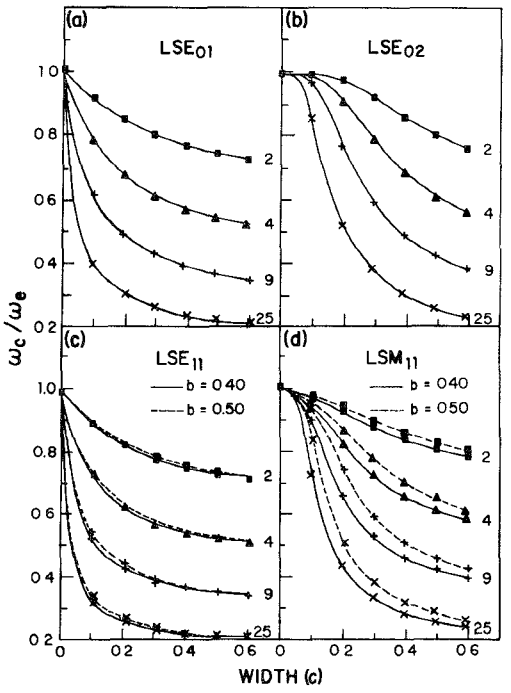

Fig. 3. Ratio of the cutoff frequency of a centrally loaded guide to that of an empty one versus the slab's width.

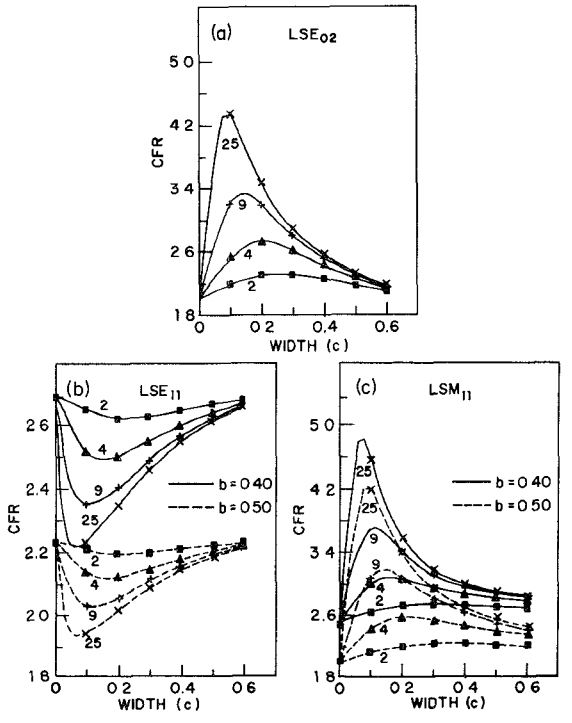

Fig. 4. Cutoff frequency ratio versus slab's width.

minimum for LSE_{11} modes. For LSE_{11} and LSM_{11} modes, CFR decreases, given ϵ and c, as b increases.

It can be seen from Figs. 4(a) and 4(b), that *for a given* b, an increase in ϵ increases the maximum CFR for the LSE_{02} mode and decreases the minimum CFR for the LSE_{11} mode. The optimal bandwidth in the guide $(\omega_{sd}/\omega_d)_{opt}$ could therefore depend on both. Fig. 5(a)

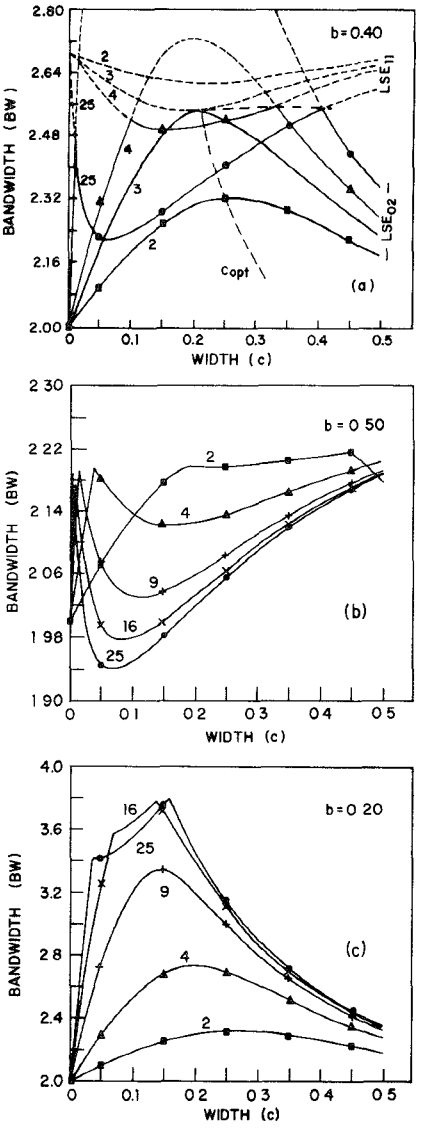

Fig. 5. Bandwidth versus slab's width.

contains a graphical superposition describing the CFR variation of both modes as a function of c, i.e., the BW dependence on c, for $b=0.40$ and $\epsilon=2$, 3, 4, and 25.

The graph obviates the fact that for $\epsilon<3$, the guide's bandwidth is determined by the LSE_{02} mode since $CFR(LSE_{11}) > CFR(LSE_{02})$ (for $\epsilon=2$, $BW_{opt} = CFR_{max}(LSE_{02})=2.32$ at $c=0.26$). For $\epsilon>3$, the bandwidth is determined by the LSE_{02} mode for $0<c<c'$ and $c''<c<1$, since in these ranges $CFR(LSE_{11}) > CFR(LSE_{02})$, and by the LSE_{11} mode for $c'<c<c''$, since in this range the inequality changes sides, c' and c'' being the crossover points of the $CFR(LSE_{02})$ and $CFR(LSE_{11})$ curves. The bandwidth variation has, therefore, always two peaks, the stronger of which determines BW_{opt} (for $\epsilon=4$, $BW_{opt}=2.56$ at $c''=0.33$). The maximum on the right has been found consistently to be the highest. For the intermediate relative permittivity $\epsilon_m = 3$, $CFR_{max}(LSE_{02})=CFR_{min}(LSE_{11})=BW_{opt}$ (for $\epsilon=3$, $BW_{opt}=2.56$ at $c=0.22$). Evidently, ϵ_m is a function of b. Figs.

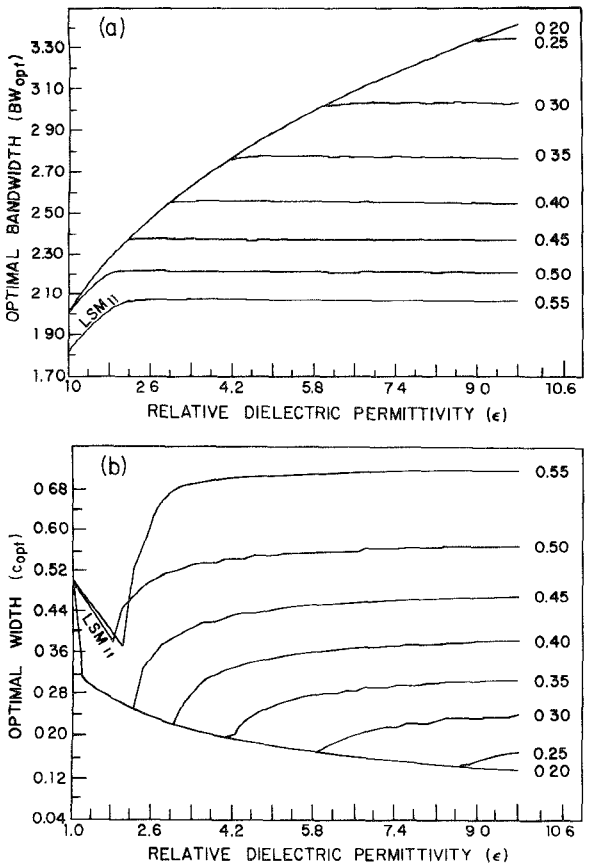

Fig. 6. Optimal bandwidth and optimal slab width versus relative permittivity.

5(b) and (c) are similar to Fig. 5(a), but with $b=0.50$ and 0.20, respectively.

Let $c_{opt}(b,\epsilon)$ denote the optimal slab width (e.g., in the cited example, $c_{opt}(0.4,2)=0.26$, $c_{opt}(0.4,3)=0.22$, and $c_{opt}(0.4,4)=0.33$). Graphs of the optimal bandwidth BW_{opt} (corresponding to c_{opt}) are given in Fig. 6(a) as a function of ϵ with b as parameter, while Fig. 6(b) describes the optimal slab width (c_{opt}) as a function of ϵ with b as parameter.

Consider, for example, $b=0.40$. It could be seen readily that in the range $1 \leqslant \epsilon \leqslant 3$ where BW_{opt} is determined by the LSE_{02} mode, it increases from 2 to 2.56 while c_{opt} decreases from 0.50 to 0.22. In the range $\epsilon \geqslant 3$ where BW_{opt} is determined by the LSE_{02} and LSE_{11} modes, it remains fairly constant and equal to 2.56, while c_{opt} increases at first and then reaches an asymptotic saturation value $c_{opt}=0.41$. This behavior could be explained with the aid of Fig. 5(a) where the optimal points have been connected. It can be seen that, as ϵ increases from 1 to 3, BW_{opt} increases and c_{opt} decreases. When ϵ becomes larger than 3, BW_{opt} remains essentially constant ($BW_{opt} \cong 2.56$), and c_{opt} increases first and then reaches an asymptotic level at 0.41. The minimum value of c_{opt} is reached, for a given b, when $\epsilon=\epsilon_m$. ϵ_m increases when b decreases, since $CFR_{min}(LSE_{11})$ increases when b decreases (Fig. 4(b)), while $CFR_{max}(LSE_{02})$ is independent of b (Fig. 4(a)).

The parameter range $b>0.50$ is of little interest in the present context, since the bandwidth cannot be substantially improved. For low ϵ and $b>0.50$, the subdominant mode is the LSM_{11} (instead of LSE_{02} for $b<0.50$).

TABLE II
RESULTS OF THE OPTIMIZATION PROCESS FOR ASYMMETRICAL SINGLE-SLAB AND SYMMETRICAL THREE-SLAB CONFIGURATIONS

Guide Loading	Prescribed Parameters	Search Parameters	Final Values of the Search Parameters	Remarks
Asymmetrical single-slab $\epsilon_1=\epsilon_3=1$	b, ϵ_2	c_2, d_2	$c_2=c_{opt}(\epsilon)$, $d_2=0$	$c_{opt}(\epsilon)$ = optimal width for a single central dielectric slab
Symmetrical three-slabs $\epsilon_1=\epsilon_5=1$ $\epsilon_2=\epsilon_4$ $c_2=c_4$	b, ϵ_3 $c_3=c_{opt}(\epsilon_3)$	ϵ_2, c_2	$\epsilon_2 \to 1$, c_2 arbitrary or $c_2 \to 0$, ϵ_2 arbitrary	"
"	b, $\epsilon_2=\epsilon_M$ $c_2=\frac{c_{opt}(\epsilon_2)}{2}$	ϵ_3, c_3	$c_3 \to 0$, ϵ_3 arbitrary	
"	b	ϵ_3, c_3 ϵ_2, c_2	$\epsilon_3=\epsilon_M$, $c_3=c_{opt}(\epsilon_M)$ $c_2 \to 0$, ϵ_2 arbitrary or $\epsilon_3=\epsilon_M$, $c_3=c_{opt}(\epsilon_M)$ $\epsilon_2 \to 1$, c_2 arbitrary or $\epsilon_3=\epsilon_2=\epsilon_M$ $c_3+2c_2=c_{opt}(\epsilon_M)$ or $c_3=0$, ϵ_3 arbitrary $\epsilon_2=\epsilon_M$, $2c_2=c_{opt}(\epsilon_M)$	The mode of convergence of the search parameters depends on their starting values. Constraint: $\epsilon_3, \epsilon_2 \leq \epsilon_M$

B. Multidielectric Slabs

We saw in the preceding section that a centrally loaded waveguide with a single dielectric slab possesses an optimum bandwidth for a given relative permittivity or prescribed height. The question arises whether or not added dielectric slabs (of different relative permittivity and width), and/or the alteration of structure symmetry, could further improve the bandwidth.

The optimization program was run repeatedly for various values of the prescribed parameters as well as initial values of the search parameters. The optimum bandwidth of an asymmetrical single slab and of a symmetrical three-slab configuration were obtained. The relative permittivity $\epsilon(x)$ was ascribed an upper bound which we denoted by ϵ_M.

The results of the optimization process are summarized in Table II. It was found that no improvement over the single centrally loaded slab configuration can be achieved. Indeed, the generalized configurations (Table II) have always degenerated to this basic structure. This conclusion is not unexpected.

C. Power Handling Capacity and Attenuation Constraints

The discussion in Section IV-A reveals the basic process of bandwidth widening whereby a lowering of b and an increase in ϵ are required. Unfortunately, the very same process would diminish the power handling capacity of the device and enhance the attenuation per unit length. This section deals with the task of achieving an optimal bandwidth (about some center frequency) constrained by

prescribed minimum power handling capacity and/or prescribed maximum acceptable losses. Conversely, for a desired and predetermined bandwidth, we may try to maximize power handling capacity or minimize attenuation.

The power carried along the guide by the dominant mode is given by [2]

$$P_z = \frac{1}{2}\,\mathrm{Re}\int_0^a\int_0^b (\bar{E}\times\bar{H}^*)\cdot\bar{a}_z\,dx\,dy = \frac{A}{2}\omega\mu_0 b\beta^3\int_0^a \phi_h^2(x)\,dx \tag{23}$$

where A is an amplitude constant. The maximum power flow is determined by the breakdown electric field ($E_{bd}(x,\omega)$), the guide's geometrical dimensions (a,b), the relative permittivity (ϵ), and the frequency (ω). We assume that breakdown occurs at the air–dielectric interface.

The power per unit length absorbed in the guide's walls due to their finite conductivity (σ) is given by [2]

$$P_c = \frac{R_m}{2}\iint_S \bar{H}_t\cdot\bar{H}_t^*\,dS \tag{24}$$

where $R_m = \sqrt{\omega\mu_0/2\sigma}$, $\bar{H}_t$ is the magnetic field component (assuming no losses) tangential to the walls, and the integration ranges over the surface of the walls. If we assume that the losses are small, perturbation theory yields

$$P_c = \frac{A\beta^2 R_m}{2}\left\{\left[\left(\frac{d\phi_h(0)}{dx}\right)^2+\left(\frac{d\phi_h(a)}{dx}\right)^2\right]b + 2\int_0^a\left[(\beta\phi_h(x))^2+\left(\frac{d\phi_h(x)}{dx}\right)^2\right]dx\right\}. \tag{25}$$

The attenuation constant will be given by [2]

$$\alpha_c = \frac{P_c}{2P_z}. \tag{26}$$

Let us define the normalized power handling capacity and the normalized attenuation constant by

$$\bar{P}_{\max} = \frac{P_{\max}(\omega)}{P'_{\max}(\omega')} \tag{27}$$

$$\bar{\alpha}_c = \frac{\alpha_c(\omega)}{\alpha'_c(\omega')} \tag{28}$$

where the primed quantities refer to the unloaded waveguide of dimensions $a=1$ and $b=0.50$ which has been chosen (rather arbitrarily) for normalization purposes. Let us define the nominal working frequencies by

$$\omega = \sqrt{\omega_d\cdot\omega_{sd}} \tag{29}$$

$$\omega' = \sqrt{\omega'_d\cdot\omega'_{sd}} \tag{30}$$

and set $\omega=\omega'$ for comparison purposes.

Graphs of $\bar{P}_{\max}$ and $\bar{\alpha}_c$ are given in Figs. 7(a) and (b) as a function of ϵ with b as parameter and $c = c_{\mathrm{opt}}(\epsilon, b)$.

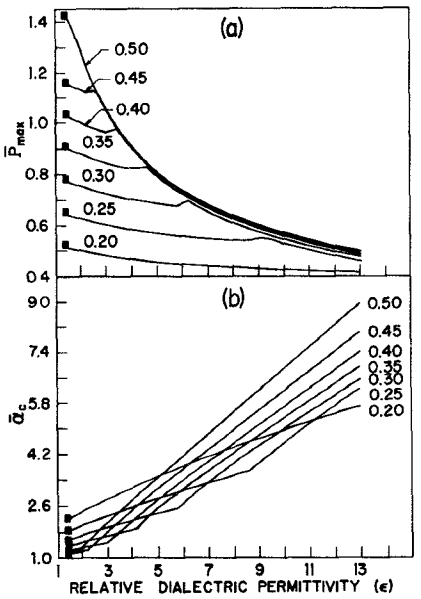

Fig. 7. Normalized power handling capacity and normalized attenuation constant versus relative permittivity.

It can be seen from Fig. 7 that, for a given ϵ, $\bar{P}_{\max}$ decreases with b (i.e., the power handling capacity decreases as the bandwidth increases). $\bar{\alpha}_c$ first decreases with b (this will not constrain the bandwidth optimization process) up to a certain $b=b_m$ corresponding to $\epsilon=\epsilon_m$, and then increases as b decreases. We may conclude that the combined requirement of optimal bandwidth together with a maximum power handling capacity and a minimum attenuation constant leads to the most advantageous choice: $b=b_m$, $\epsilon=\epsilon_m$, and $c=c_{\mathrm{opt}}(\epsilon_m, b_m)$ of the waveguide parameters. An analysis made taking into consideration dielectric losses left this conclusion unchanged.

References

[1] P. H. Vartanian, W. P. Ayres, and A. L. Helgesson, "Propagation in dielectric slab loaded rectangular waveguide," *IRE Trans. Microwave Theory Tech.*, vol. MTT-6, pp. 215–222, Apr. 1958.

[2] R. E. Collin, *Field Theory of Guided Waves*. New York: McGraw-Hill, 1960.

[3] F. E. Gardiol, "Higher-order modes in dielectrically loaded rectangular waveguides," *IEEE Trans. Microwave Theory Tech.*, vol. MTT-16, pp. 919–924, Nov. 1968.

[4] T. K. Findakly and H. M. Haskal, "On the design of dielectric loaded waveguides," *IEEE Trans. Microwave Theory Tech.*, vol. MTT-24, pp. 39–43, Jan. 1976.

[5] R. F. Harrington, *Field Computation by Moment Methods*. New York: Macmillian, 1968.

[6] M. J. D. Powell, "An efficient method for finding the minimum of function of several variables without calculating derivatives," *Comput. J.*, vol. 7, pp. 155–162, 1964.

[7] J. A. Nelder and R. Mead, "A simplex method for function minimization," *Comput. J.*, vol. 7, pp. 308–313, 1965.

[8] L. B. Felsen and N. Marcuvitz, *Radiation and Scattering of Waves*. Englewood Cliffs, NJ: Prentice-Hall, 1973.

[9] J. W. Dettman, *Mathematical Methods in Physics and Engineering*. New York: McGraw-Hill, 1969.

[10] R. F. Harrington, *Time-Harmonic Electromagnetic Fields*. New York: McGraw-Hill, 1961.

[11] R. Mittra, Ed., *Computer Techniques for Electromagnetics*. Oxford, England: Pergamon, 1973.

[12] S. G. Mikhlin, *Variational Methods in Mathematical Physics*. New York: Macmillan, 1964.